Supplementary Information

Designing the water-quenching resistant high luminescent europium complexes by regulating the orthogonal arrangement of bis-β-diketone ligands

Mei Li, Yanyan Zhou, Yuan Yao, Ting Gao, Pengfei Yan,* and Hongfeng Li*

Key Laboratory of Functional Inorganic Material Chemistry, Ministry of Education, P. R. China; School of Chemistry and Materials Science, Heilongjiang University, Harbin 150080, P. R. China.

Experimental Section.

Synthesis of $Gd_2(BTDA)_3$.

To a 7 mL methanol solution of 1,8-bis(4,4,4-trifluoro-1,3-dioxobutyl)anthracene BTDA (0.10 g, 0.22 mmol), Et_3N (0.05 g, 0.44 mmol) was added, and the mixture was allowed to stir for 5 min. To this solution, $GdCl_3 \cdot 6H_2O$ (0.06 g, 0.15 mmol) in methanol (3 mL) was added dropwise and refluxed under reflux for 2 h. The product was filtered and washed with H_2O (2 × 10 mL) and dried under vacuum to give the desired product.

$Gd_2(BTDA)_3$. Yield: 83%. Anal. Calc. for $C_{66}H_{30}F_{18}O_{12}Gd_2$ (1671.43): C, 47.43; H, 1.81. Found: C, 47.61; H, 1.99. ESI-MS: *m/z* = 1672.4331 $[Gd_2(\mathbf{BTDA})_3 + H]^+$.

Synthesis of $(HNEt_3)[Ln(BTFA)_4]$.

To a solution of Ligand 4,4,4-trifluoro-1-phenyl-2,4-butanedionate BTFA (0.10 g, 0.46 mmol) and dry Et_3N (0.09 g, 0.93 mmol) in CH_3CN (5 mL), a solution of $Ln(OTf)_3$ (Ln = Eu, Gd; 0.11 mmol) in 2 mL of CH_3CN was added while stirring, the mixture was stirred for 24 h at room temperature, and then the precipitates ware formed after the addition of water. Finally, the produce was filtered and dried in vacuum.

$(HNEt_3)[Eu(BTFA)_4]$. Yield: 81%. Anal. Calc. for $C_{46}H_{40}EuF_{12}NO_8$ (1115.18): C, 52.33; H, 3.12; N, 1.26. Found: C, 52.26; H, 3.24; N, 1.08. ^1H NMR (400 MHz, CD_3CN) δ 7.65 (d, *J* = 7.4 Hz, 2H), 7.34 (t, *J* = 7.1 Hz, 2H), 7.28 (t, *J* = 7.2 Hz, 1H), 4.80 (s, 1H). ESI-MS *m/z* = 1012.9412 $[Eu(\mathbf{BTFA})_4]^-$.

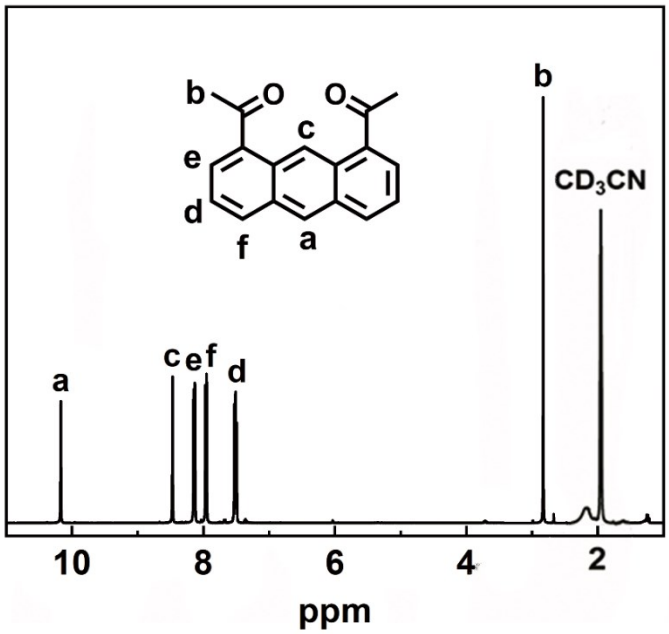

Figure S1. ^{1}H NMR spectrum of 1,8-diacetylanthracene in CD_3CN.

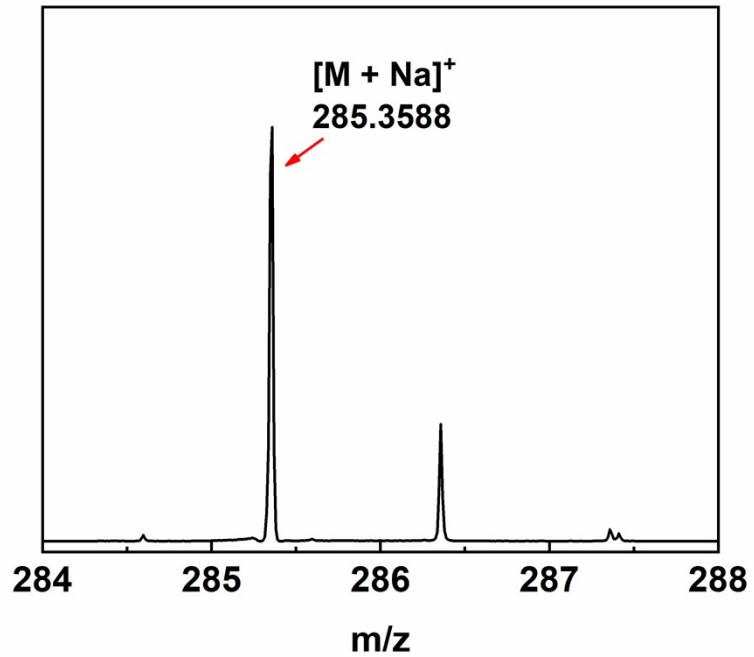

Figure S2. ESI-TOF-MS of 1,8-diacetylanthracene.

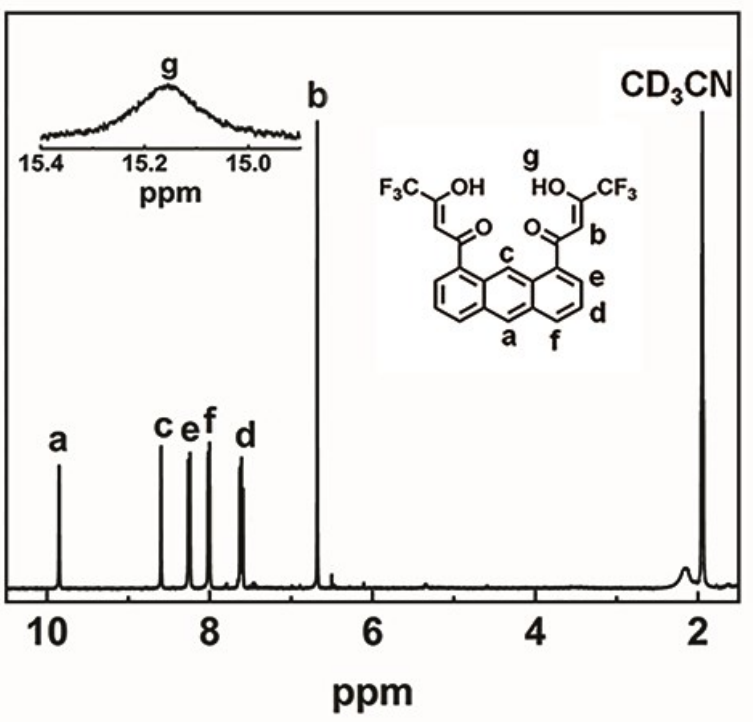

Figure S3. ^{1}H NMR spectrum of BTDA in CD_3CN.

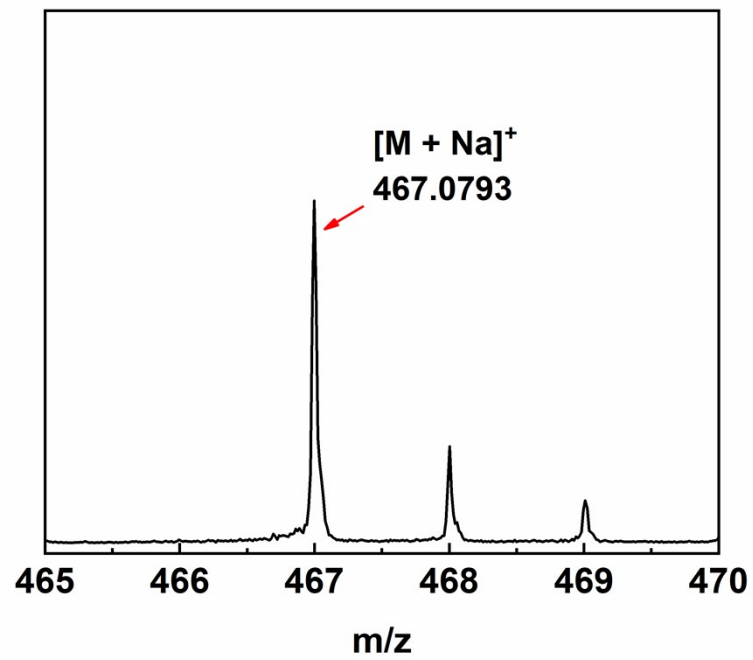

Figure S4. ESI-TOF-MS of BTDA.

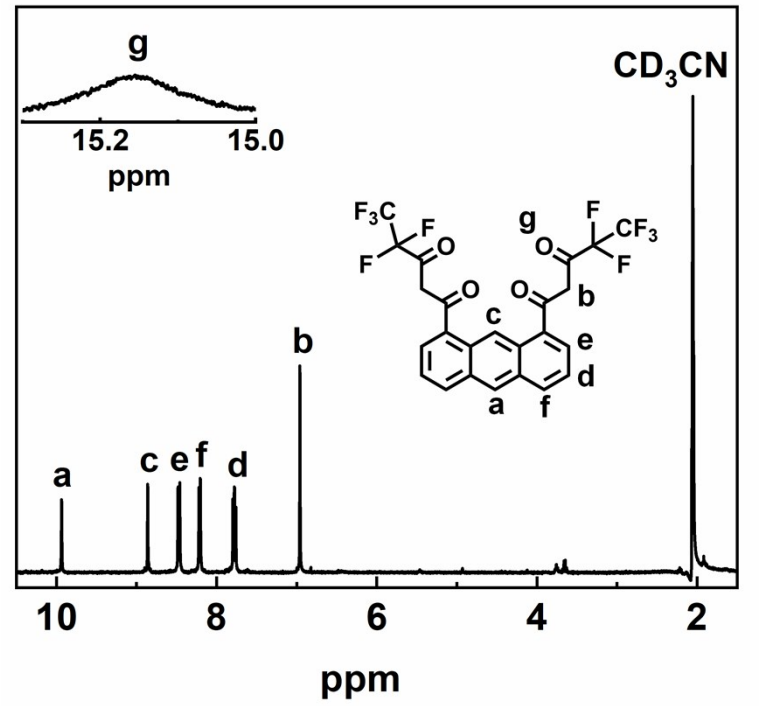

Figure S5. ^{1}H NMR spectrum of BPDA in CD_3CN.

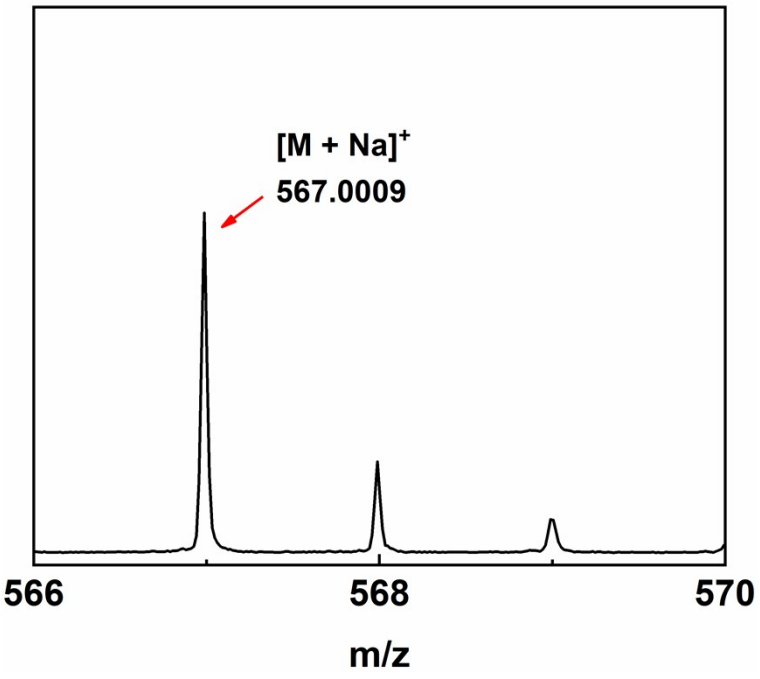

Figure S6. ESI-TOF-MS of BPDA.

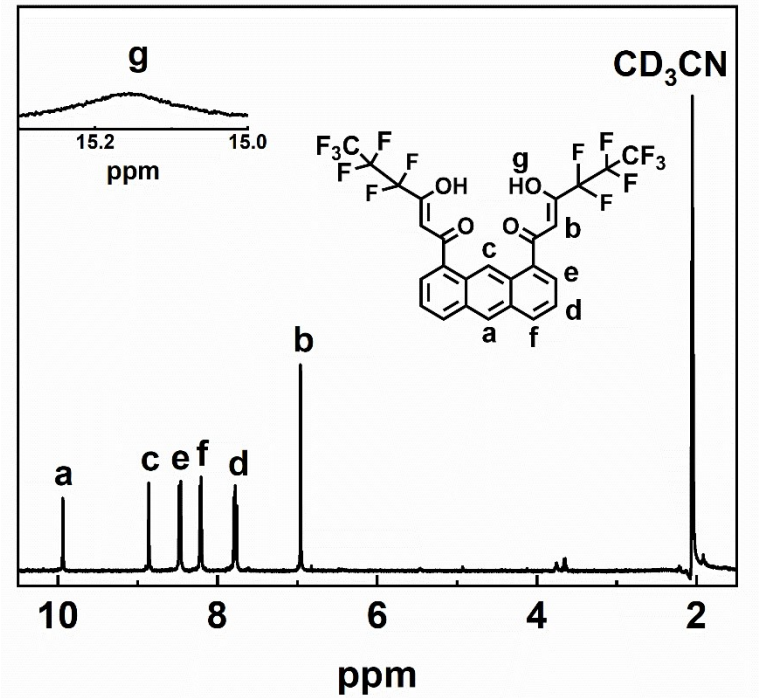

Figure S7. ^{1}H NMR spectrum of BHDA in CD_3CN.

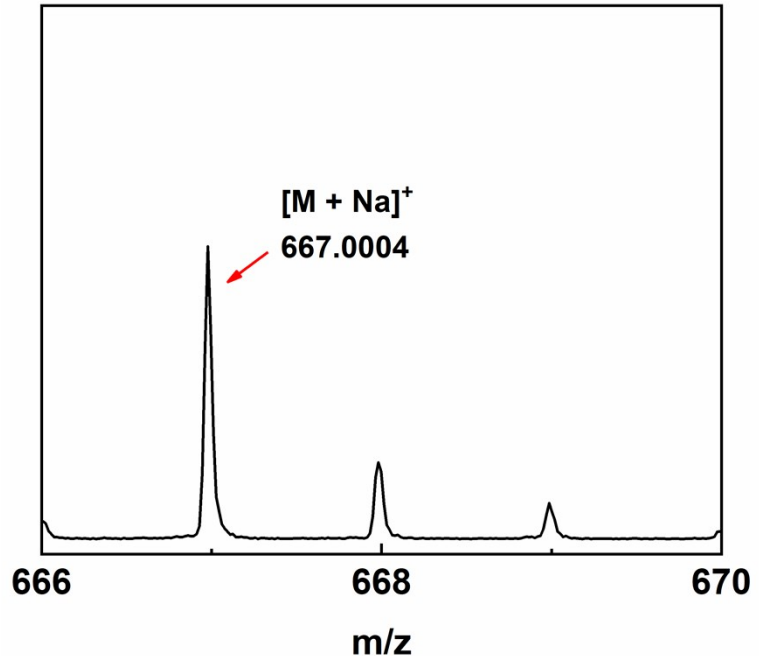

Figure S8. ESI-TOF-MS of BHDA.

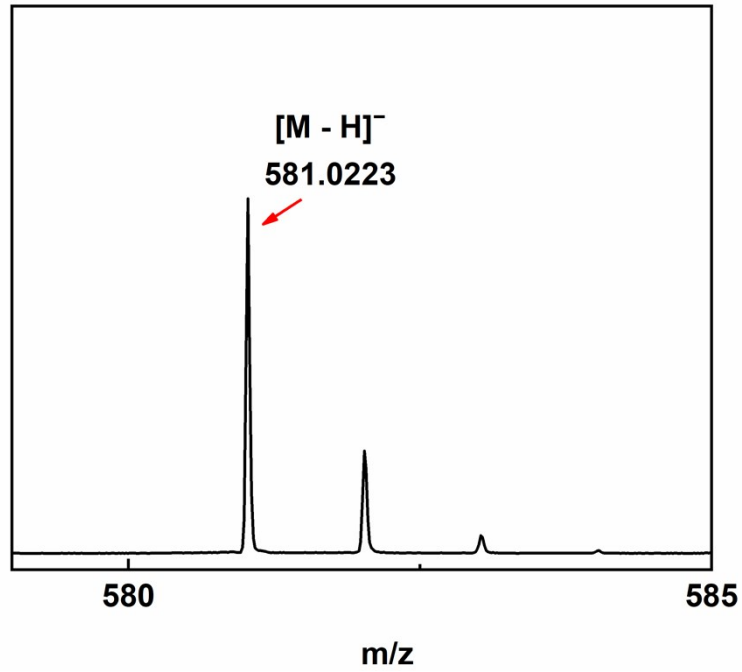

Figure S9. ESI-TOF-MS of **L**[1].

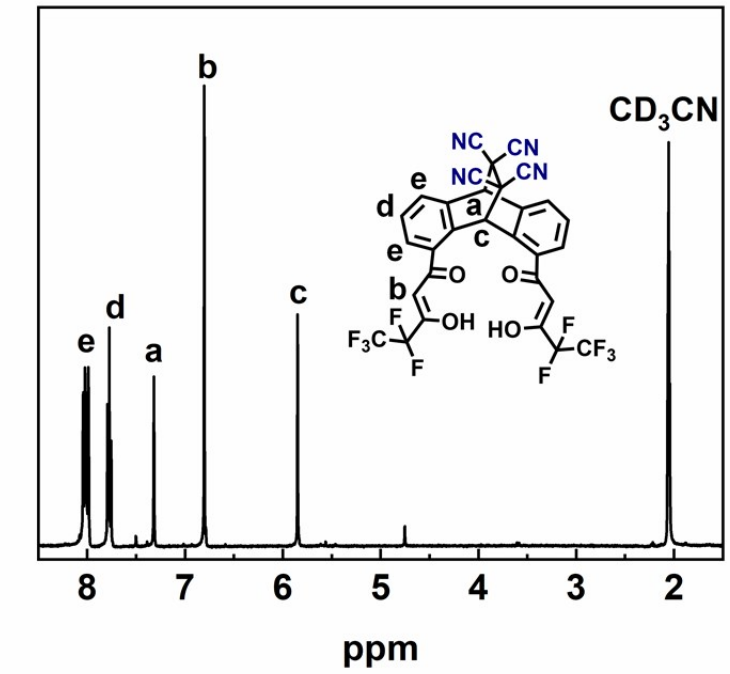

Figure S10. ^{1}H NMR spectrum of **L**[2] in CD_3CN.

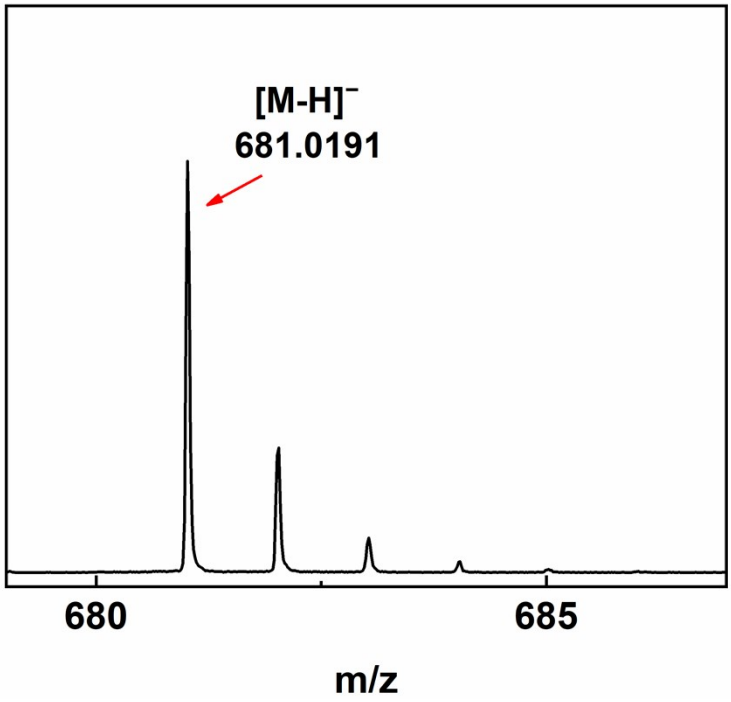

Figure S11. ESI-TOF-MS of **L²**.

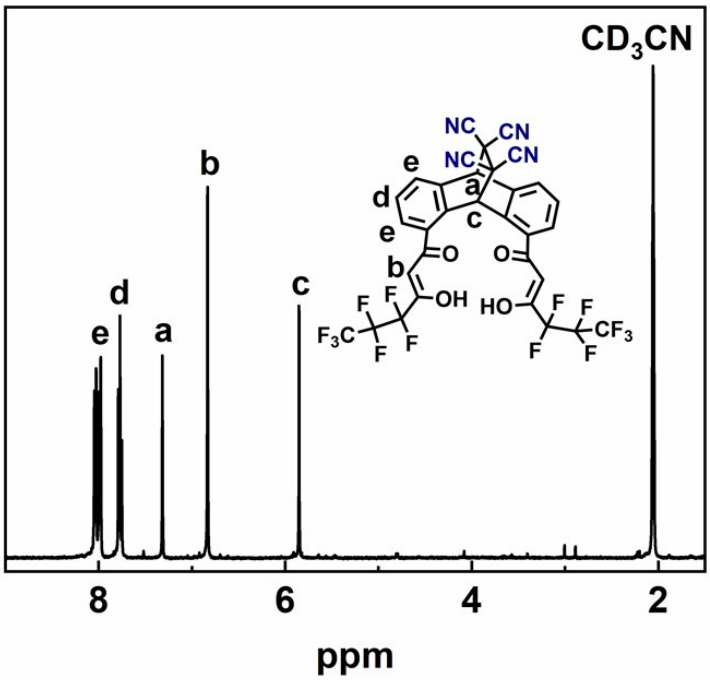

Figure S12. ^{1}H NMR spectrum of **L³** in CD_3CN.

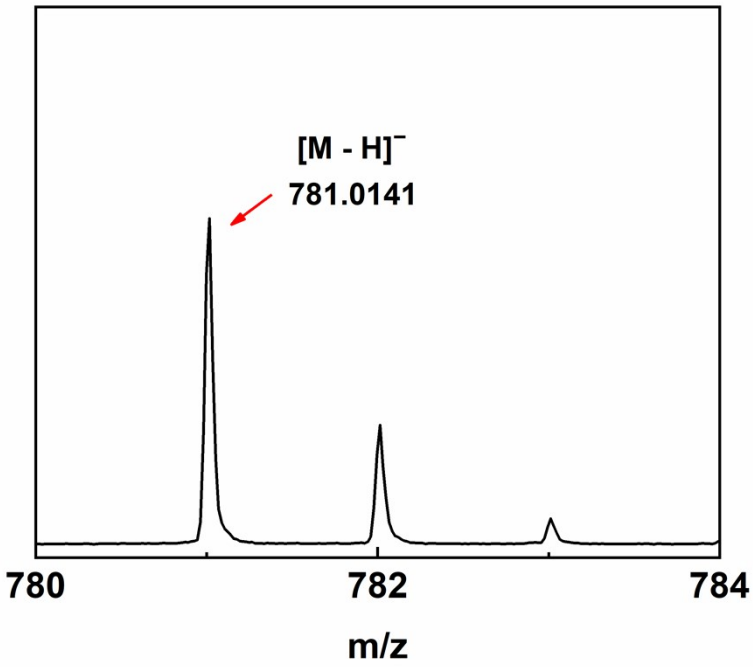

Figure S13. ESI-TOF-MS of $\mathbf{L^3}$.

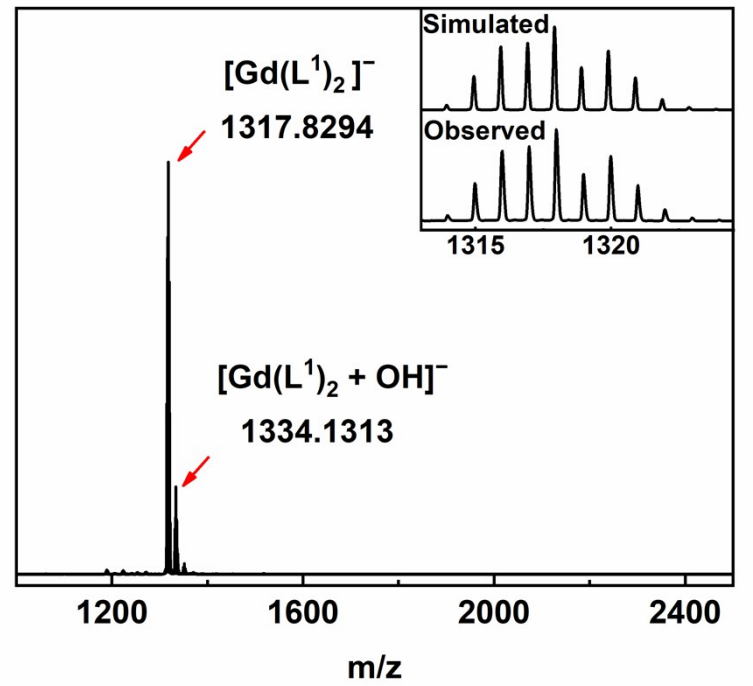

Figure S14. ESI-TOF-MS of $[Gd(\mathbf{L^1})_2]^-$.

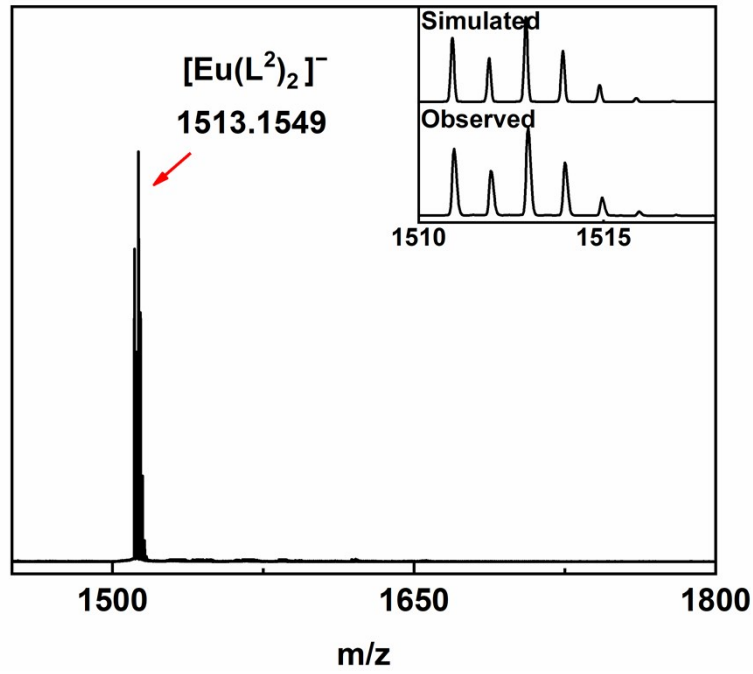

Figure S15. ESI-TOF-MS of $[Eu(\mathbf{L^2})_2]^-$.

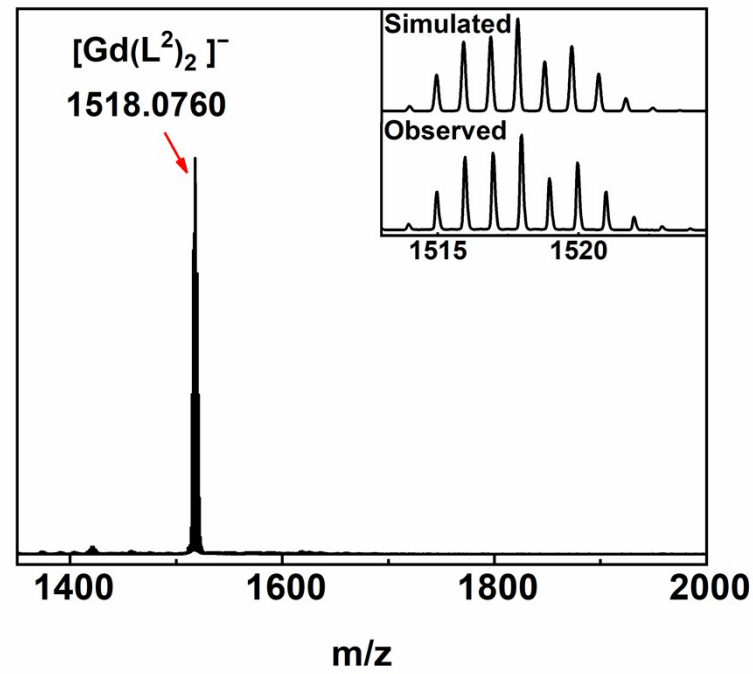

Figure S16. ESI-TOF-MS of $[Gd(\mathbf{L^2})_2]^-$.

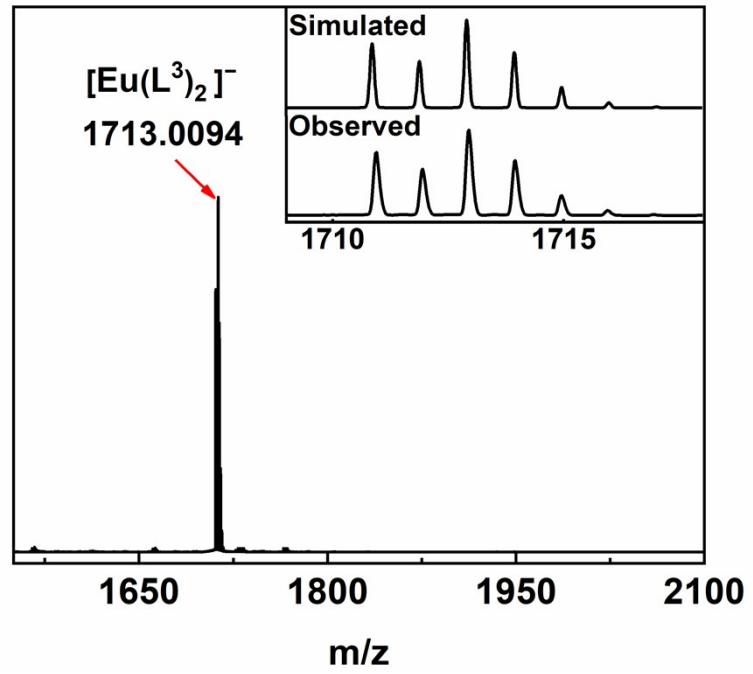

Figure S17. ESI-TOF-MS of $[Eu(\mathbf{L^3})_2]^-$.

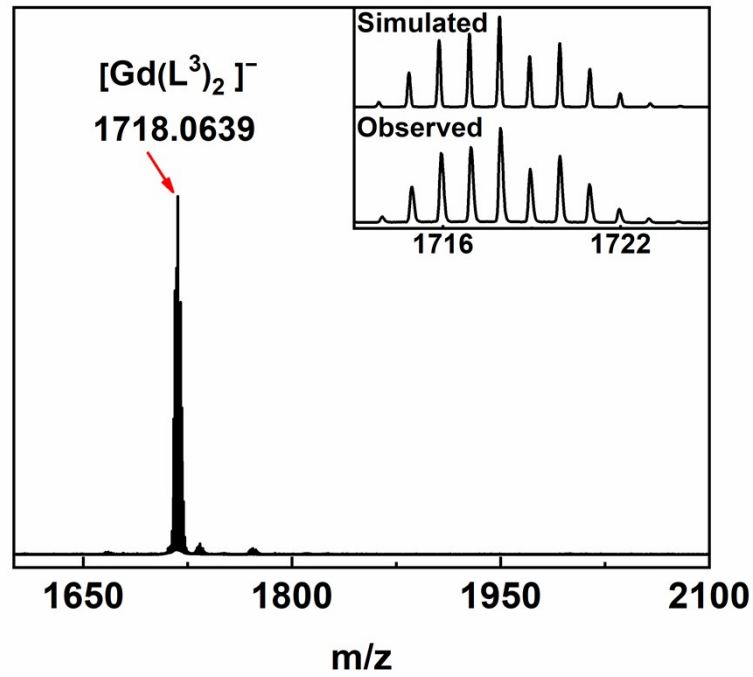

Figure S18. ESI-TOF-MS of $[Gd(\mathbf{L^3})_2]^-$.

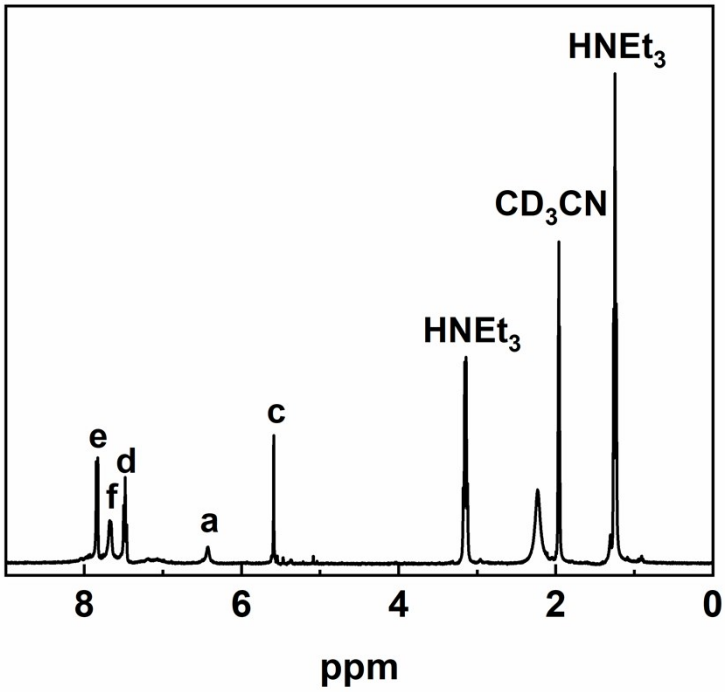

Figure S19. ^{1}H NMR spectrum of $(HNEt_3)[Eu(\mathbf{L^2})_2]$ in CD_3CN.

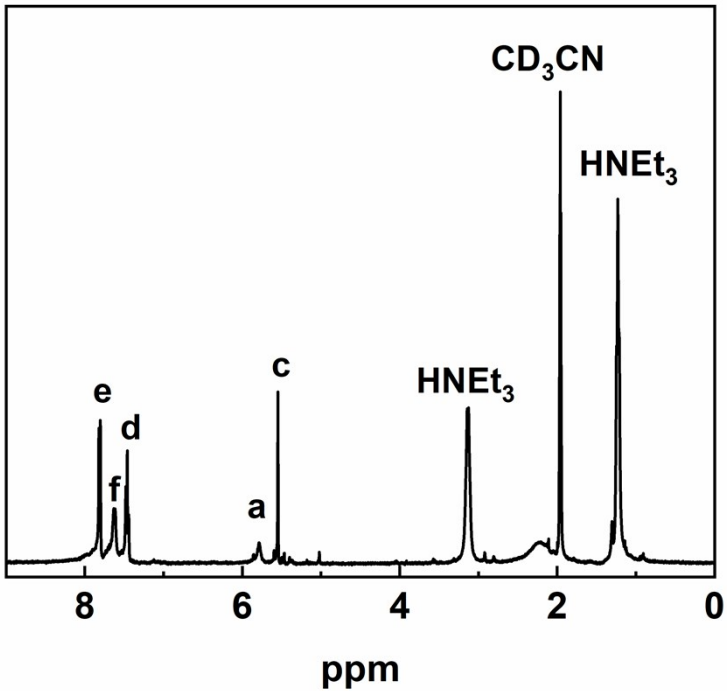

Figure S20. ^{1}H NMR spectrum of $(HNEt_3)[Eu(\mathbf{L^3})_2]$ in CD_3CN.

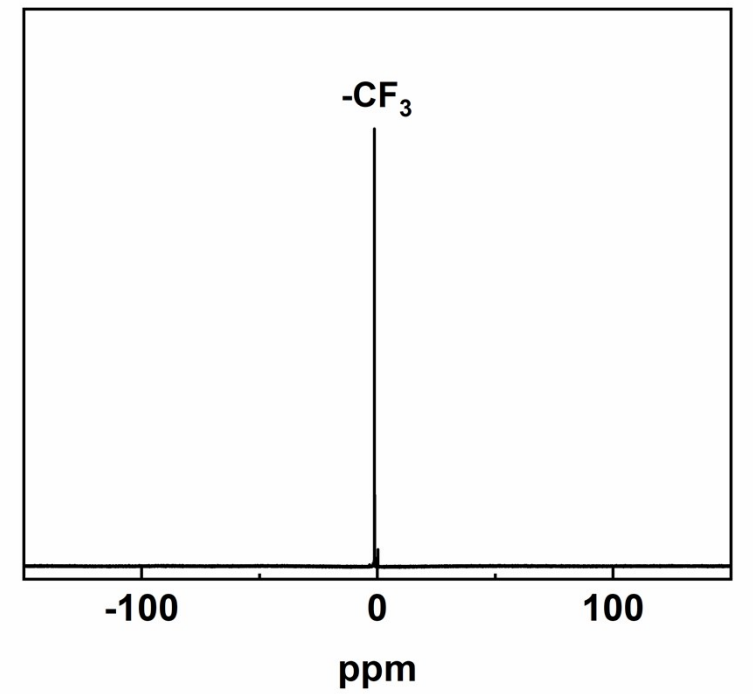

Figure S21. ^{19}F NMR spectrum of $(HNEt_3)[Eu(\mathbf{L^1})_2]$ in CD_3CN.

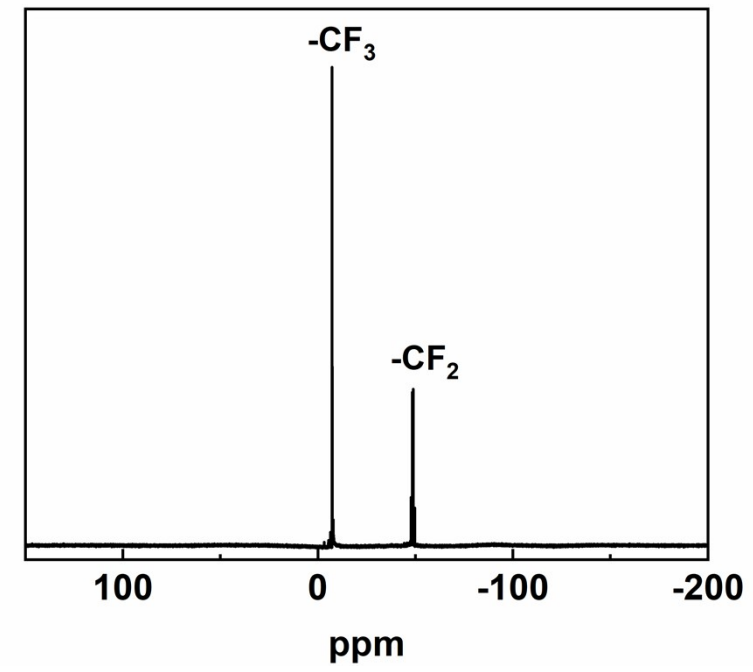

Figure S22. ^{19}F NMR spectrum of $(HNEt_3)[Eu(\mathbf{L^2})_2]$ in CD_3CN.

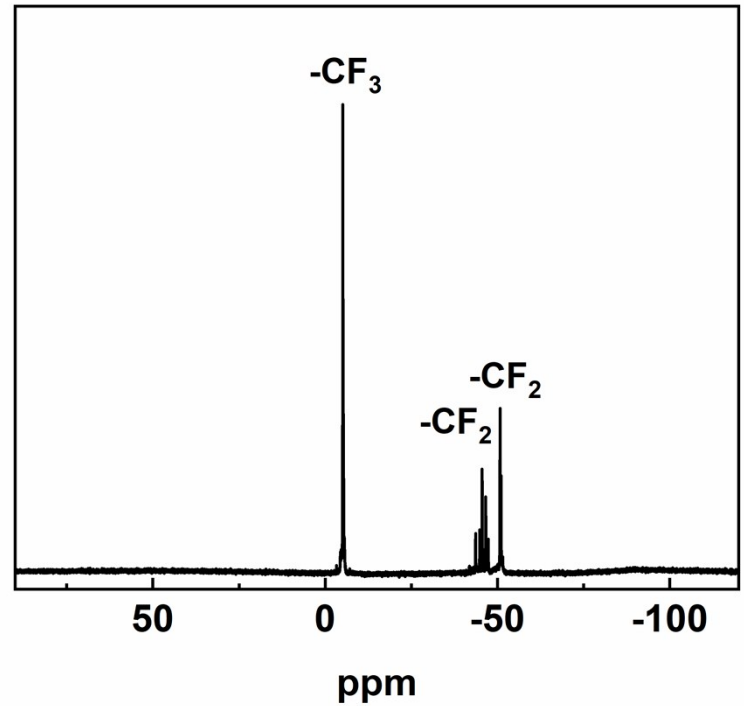

Figure S23. ^{19}F NMR spectrum of $(HNEt_3)[Eu(\mathbf{L^3})_2]$ in CD_3CN.

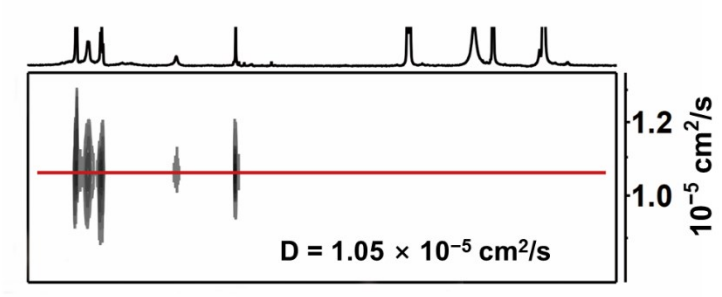

Figure S24. ^{1}H DOSY spectrum of $(HNEt_3)[Eu(\mathbf{L^2})_2]$ in CD_3CN.

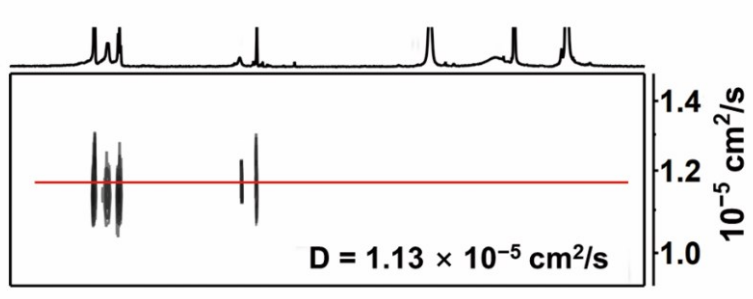

Figure S25. ^{1}H DOSY spectrum of $(HNEt_3)[Eu(\mathbf{L^3})_2]$ in CD_3CN.

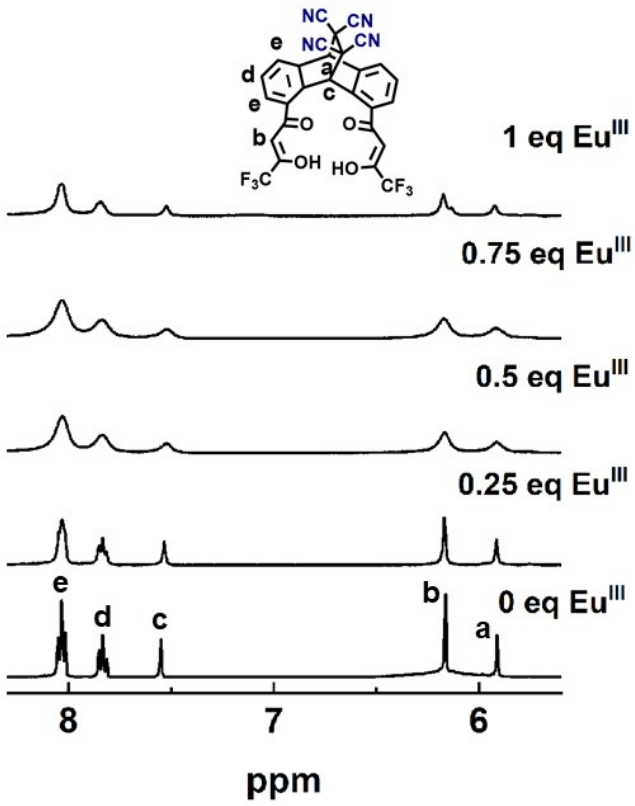

Figure S26. ^{1}H NMR spectra (400 MHz, CD_3CN) of ligand $\mathbf{L^1}$ (1.72×10^{-3} M) upon titration of $Eu(OTf)_3$ (0−1 eq.).

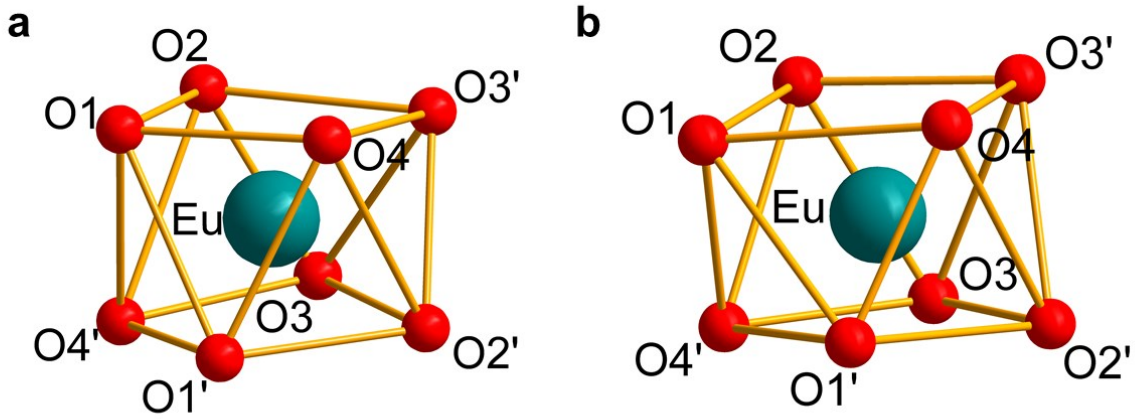

Figure S27. Coordination polyhedra of Eu^{3+} in $(HNEt_3)[Eu(\mathbf{L^1})_2]$ obtained from (a) the single crystals structure and (b) the optimized structures. By utilizing SHAPE 2.1 software, the calculated values to estimate the coordination geometry are about the same, 0.498 for obtained and 0.499 for optimized structure with D_{4d} symmetry.

Table S1. Shape analysis of europium complexes by SHAPE 2.1 software.

Complexes	Square antiprism (D_{4d})	Triangular dodecahedron (D_{2d})	Biaugmented trigonal prism (C_{2v})
the single crystals	0.498	1.879	2.426
the optimized structures	0.499	1.882	2.425
$(HNEt_3)[Eu(\mathbf{L^2})_2]$	0.539	1.643	2.543
$(HNEt_3)[Eu(\mathbf{L^3})_2]$	0.594	1.938	2.599

Table S2. Crystal data of the complex $(HNEt_3)[Eu(\mathbf{L^1})_2]$.

	$(HNEt_3)[Eu(\mathbf{L^1})_2]$
CCDC Number	2054411
formula	$C_{73}H_{58}F_{12}EuN_9O_{10}$
Mr	1601.24
cryst syst	monoclinic
space group	C2/c
a (Å)	21.0646(11)
b (Å)	13.3266(7)
c (Å)	26.5837(12)
α (deg)	90
β (deg)	99.442(2)
γ (deg)	90
V (Å^3)	7361.5(6)
Z	4
ρ (g cm^3)	1.445
μ (mm^{-1})	0.945
F (000)	3240.0
R_1,[$I > 2\sigma(I)$]	0.0375
wR_2,[$I > 2\sigma(I)$]	0.1079
R_1, (all data)	0.0385
wR_2, (all date)	0.1091
GOF on F^2	1.103

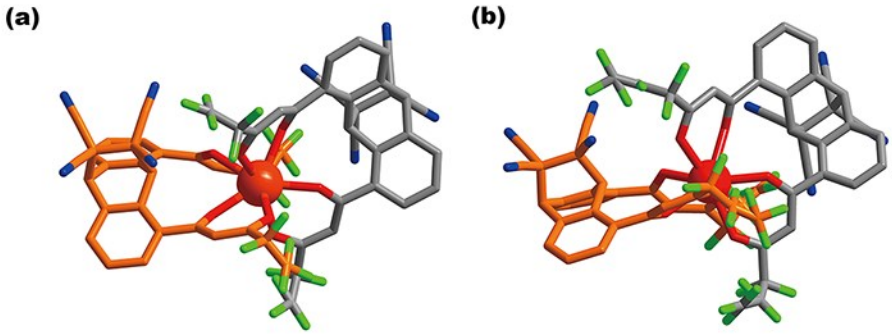

Figure S28. Sparkle/PM3 ground state geometries of (a) $(HNEt_3)[Eu(\mathbf{L^2})_2]$ and (b) $(HNEt_3)[Eu(\mathbf{L^3})_2]$.

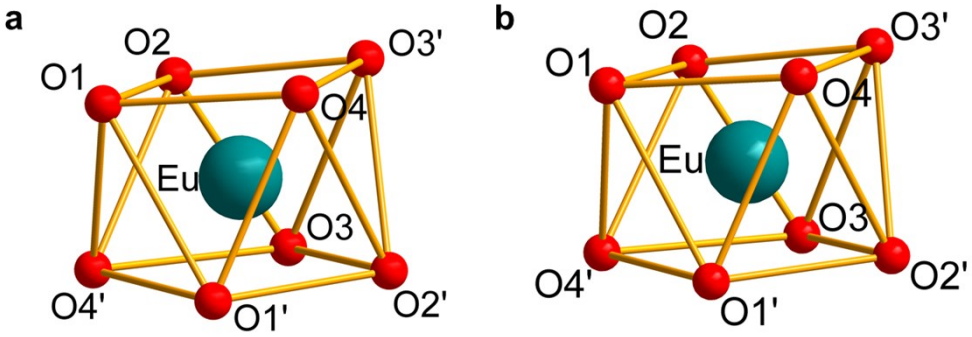

Figure S29. Coordination polyhedra of (a) $(HNEt_3)[Eu(\mathbf{L^2})_2]$ and (b) $(HNEt_3)[Eu(\mathbf{L^3})_2]$.

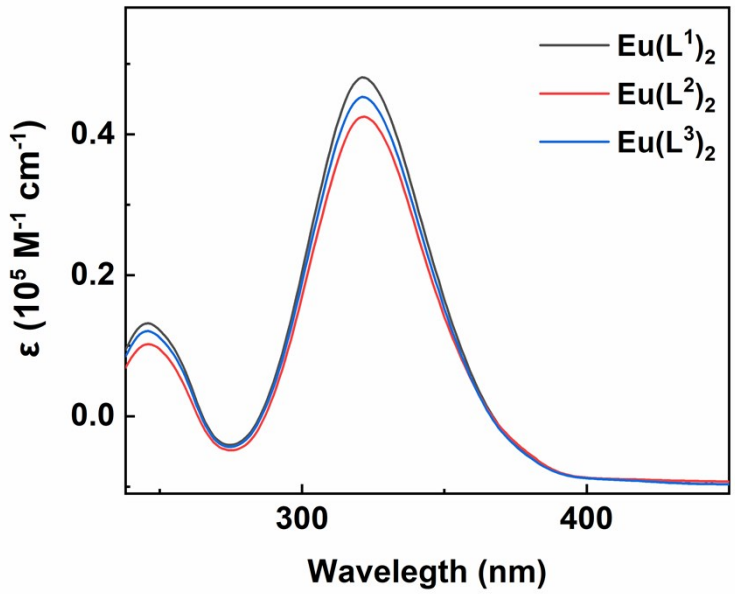

Figure S30. UV−vis absorption spectra of complexes $(HNEt_3)[Eu(\mathbf{L^1})_2]$ (black line), $(HNEt_3)[Eu(\mathbf{L^2})_2]$ (red line) and $(HNEt_3)[Eu(\mathbf{L^3})_2]$ (blue line) in a mixture of CH_3CN and water (

ν_{CH_3CN}/ν_{H_2O} = 84:16).(c = 1.0 × 10^{-5} M).

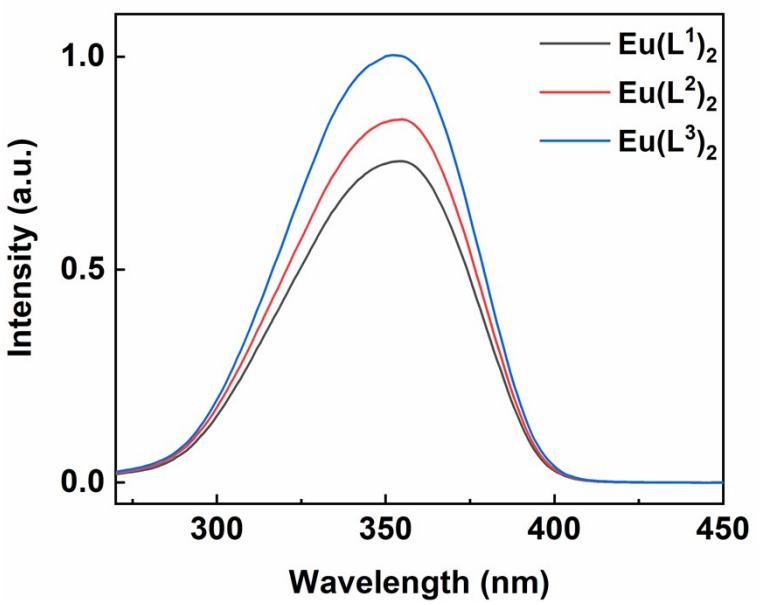

Figure S31. Excitation spectra of ($HNEt_3$)[Eu($\mathbf{L^1}$)$_2$] (black line), ($HNEt_3$)[Eu($\mathbf{L^2}$)$_2$] (red line) and ($HNEt_3$)[Eu($\mathbf{L^3}$)$_2$] (blue line) in CH_3CN (1.0 × 10^{-5} M).

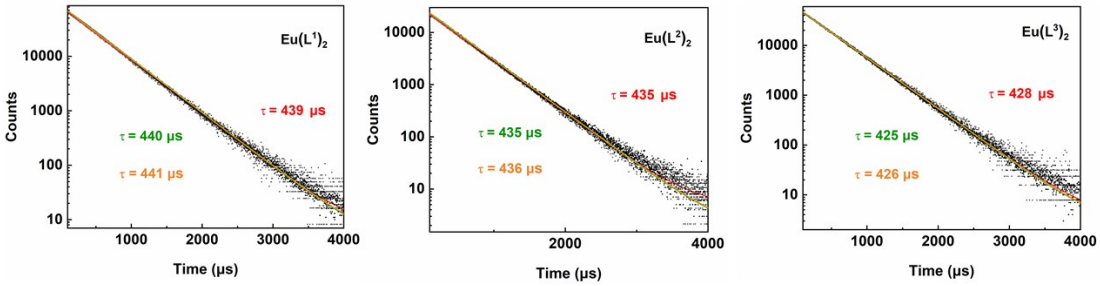

Figure S32. Luminescence decay curves of ($HNEt_3$)[Eu($\mathbf{L^1}$)$_2$] (left), ($HNEt_3$)[Eu($\mathbf{L^2}$)$_2$] (middle) and ($HNEt_3$)[Eu($\mathbf{L^3}$)$_2$] (right).

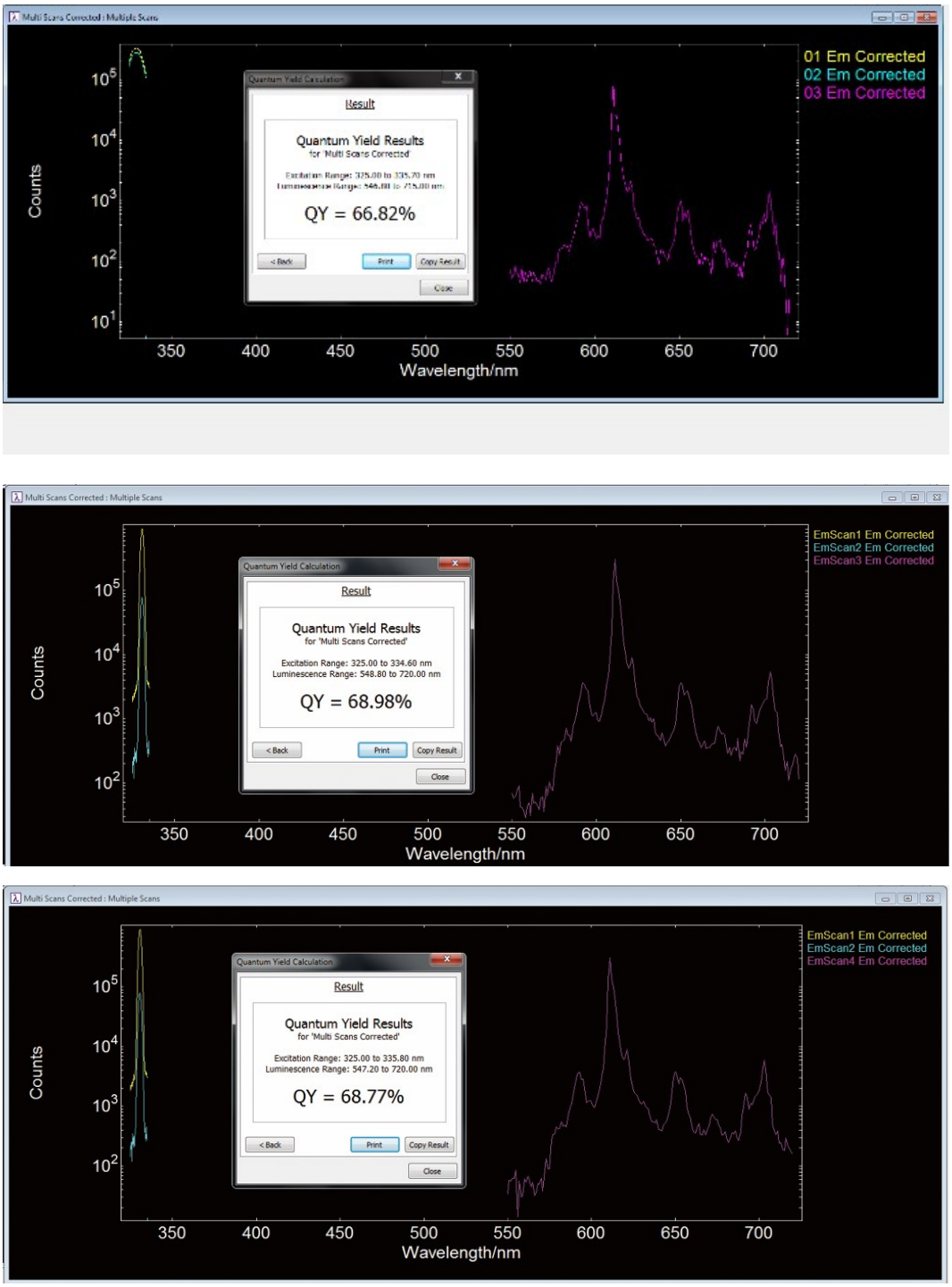

Figure S33. The screenshot of the luminescence quantum yield measurement of $(HNEt_3)[Eu(\mathbf{L^1})_2]$ in CH_3CN.

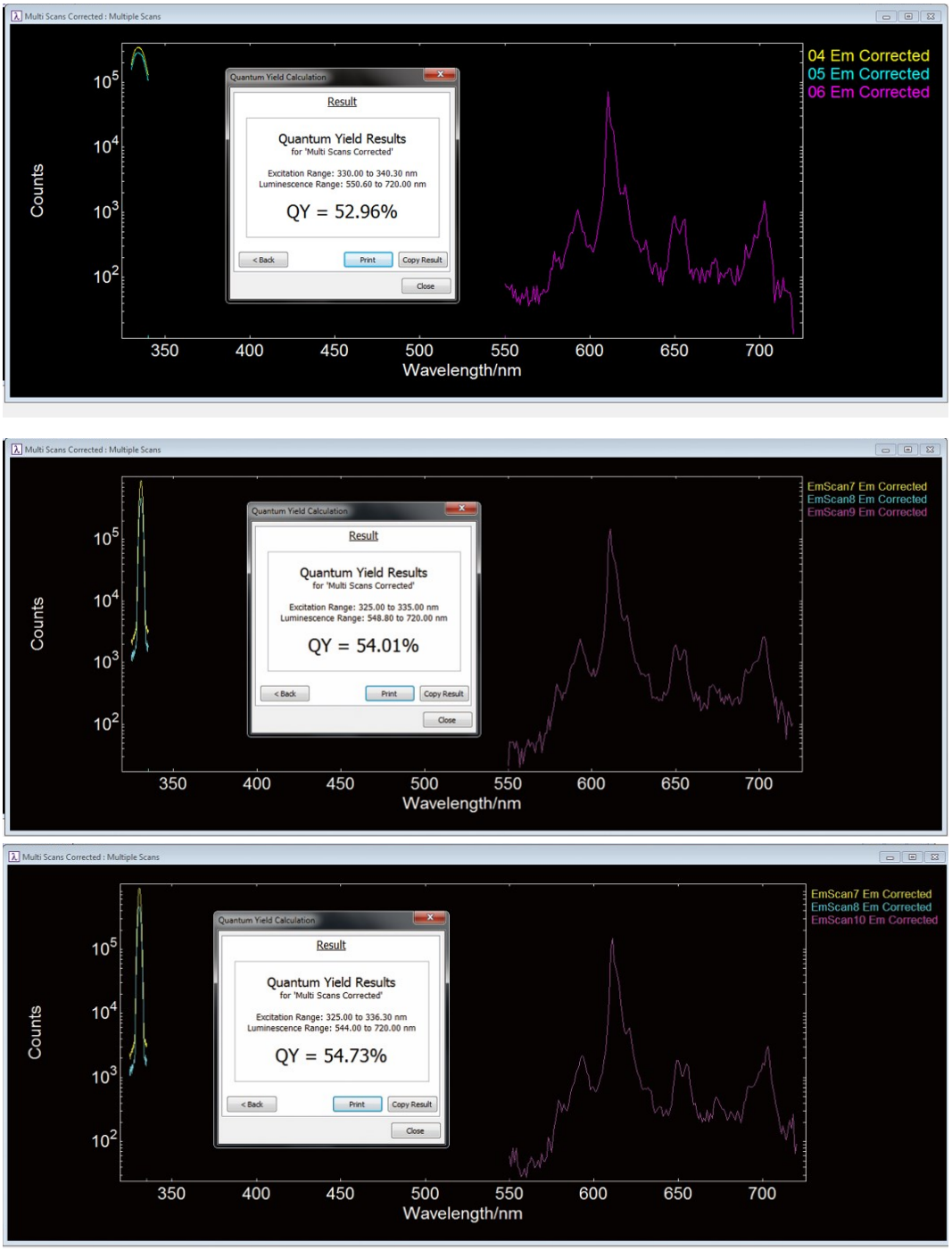

Figure S34. The screenshot of the luminescence quantum yield measurement of $(HNEt_3)[Eu(\mathbf{L^2})_2]$ in CH_3CN.

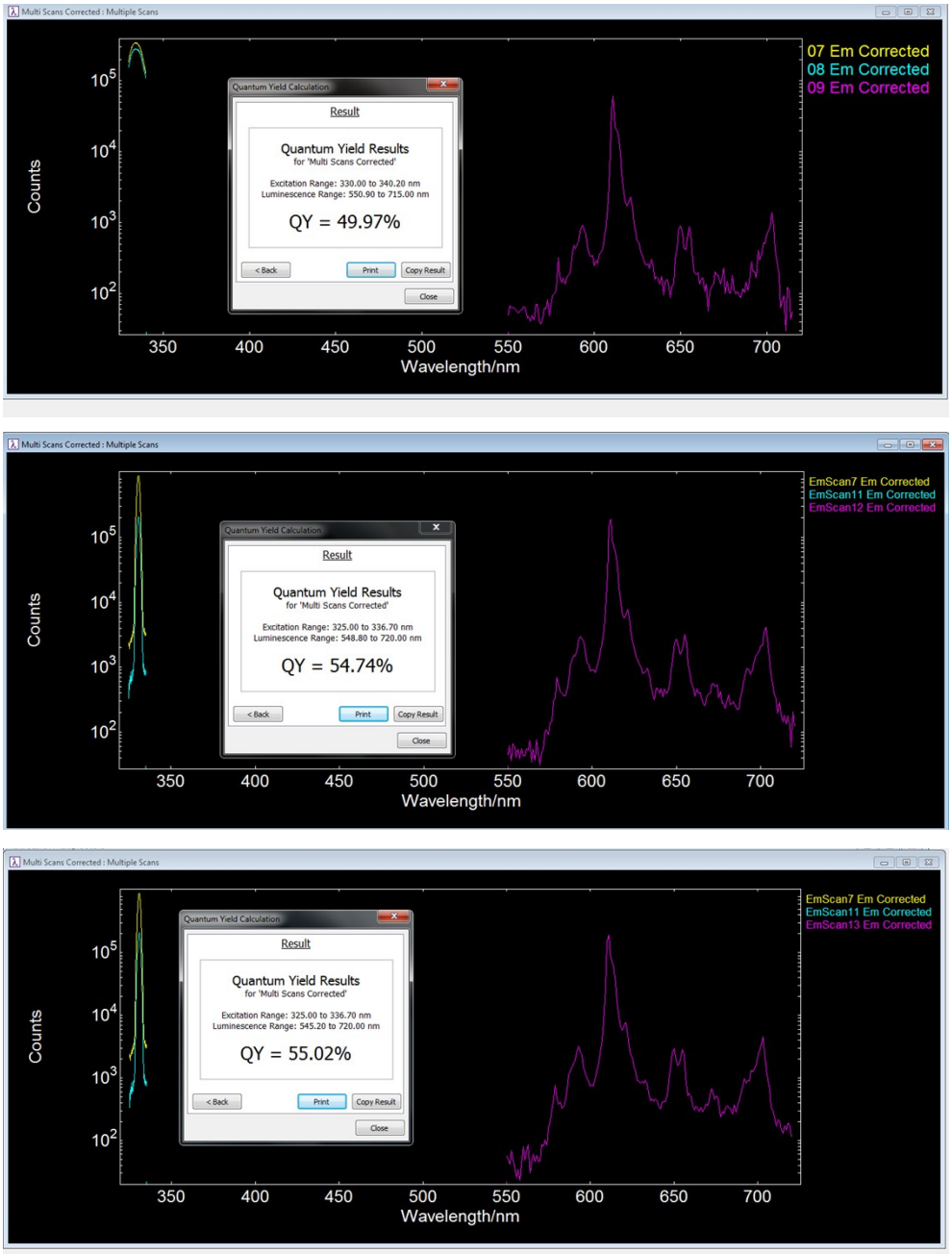

Figure S35. The screenshot of the luminescence quantum yield measurement of $(HNEt_3)[Eu(\mathbf{L^3})_2]$ in CH_3CN.

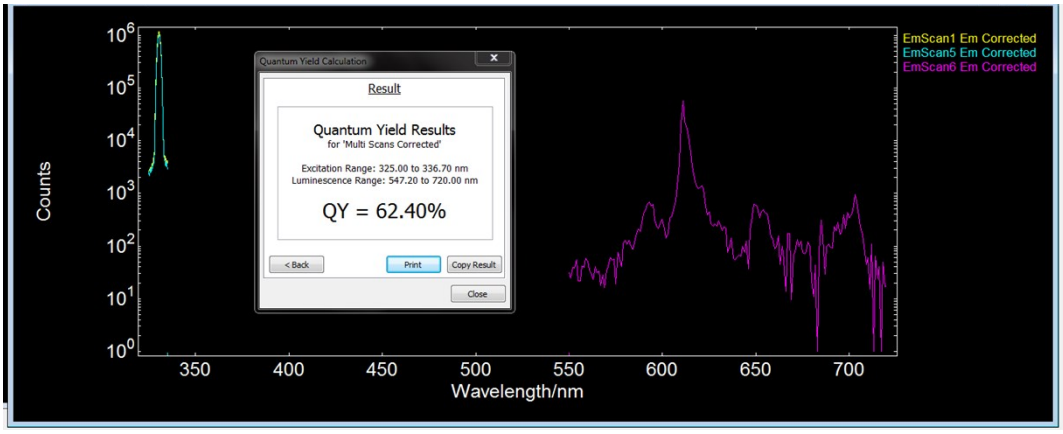

Figure S36. The screenshot of the luminescence quantum yield measurement of $(HNEt_3)[Eu(\mathbf{L^1})_2]$ in a mixture of CH_3CN and water ($^{\nu_{CH_3CN}}/_{\nu_{H_2O}}$ = 84:16).

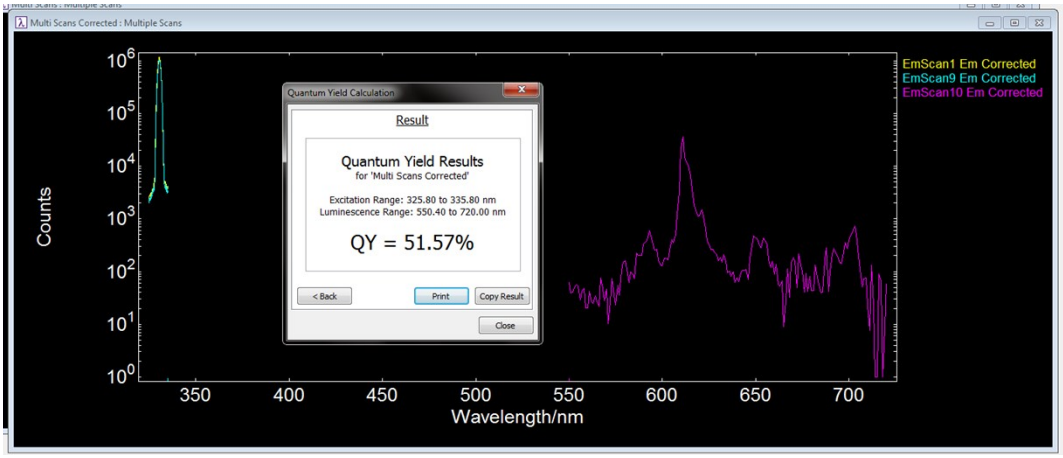

Figure S37. The screenshot of the luminescence quantum yield measurement of $(HNEt_3)[Eu(\mathbf{L^2})_2]$ in a mixture of CH_3CN and water ($^{\nu_{CH_3CN}}/_{\nu_{H_2O}}$ = 84:16).

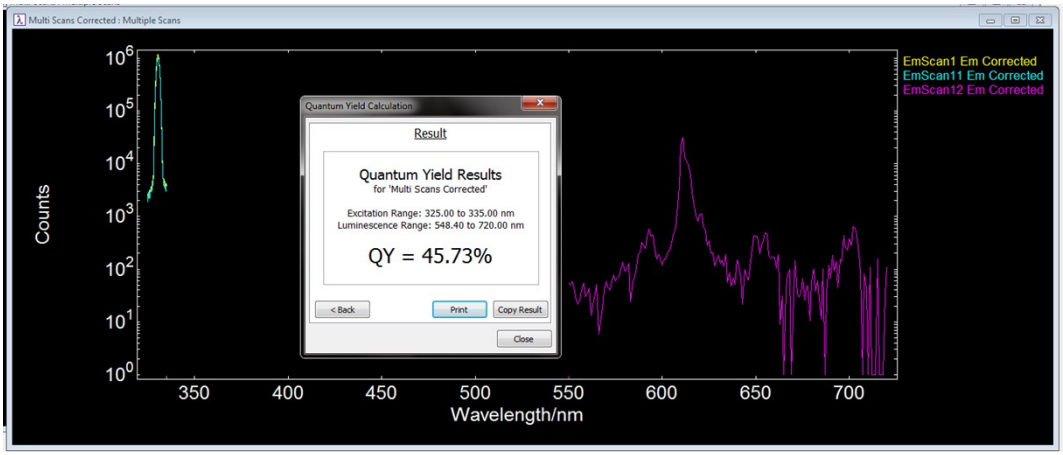

Figure S38. The screenshot of the luminescence quantum yield measurement of $(HNEt_3)[Eu(\mathbf{L^3})_2]$ in a mixture of CH_3CN and water ($^{\nu_{CH_3CN}}/_{\nu_{H_2O}}$ = 84:16).

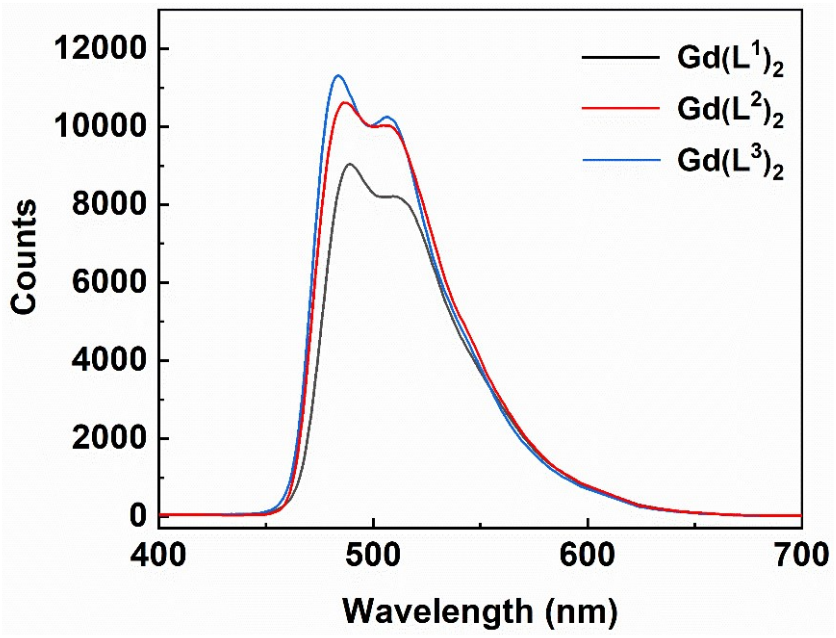

Figure S39. Phosphorescence spectra of $(HNEt_3)[Gd(\mathbf{L^1})_2]$ (black line), $(HNEt_3)[Gd(\mathbf{L^2})_2]$ (red line) and $(HNEt_3)[Gd(\mathbf{L^3})_2]$ (blue line) in THF at 77 K.

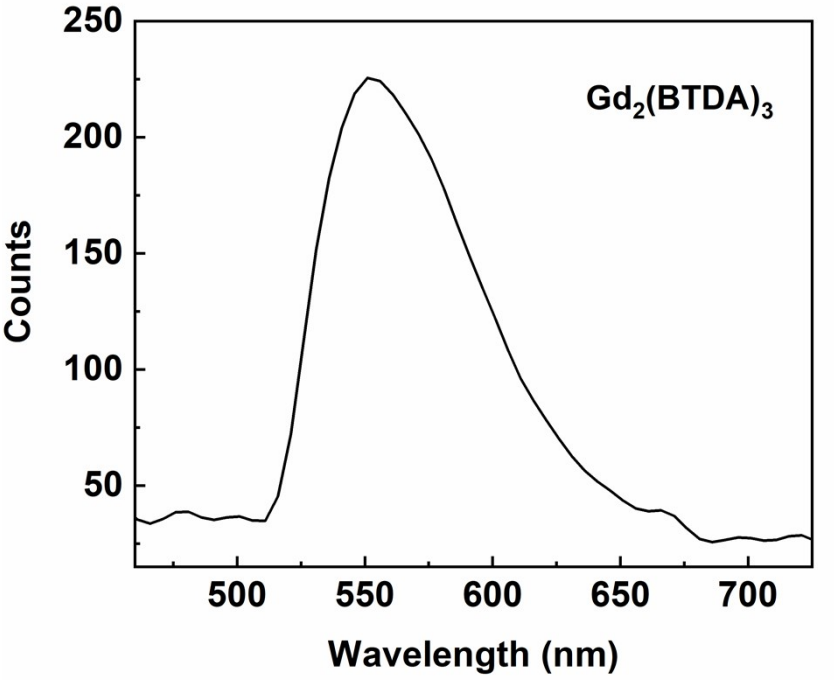

Figure S40. Phosphorescence spectra of $Gd_2(\mathbf{BTDA})_3$ in a mixture of CH_3CN and CH_3OH ($\nu_{CH_3CN}/\nu_{CH_3OH}$ = 1:1) at 77 K.

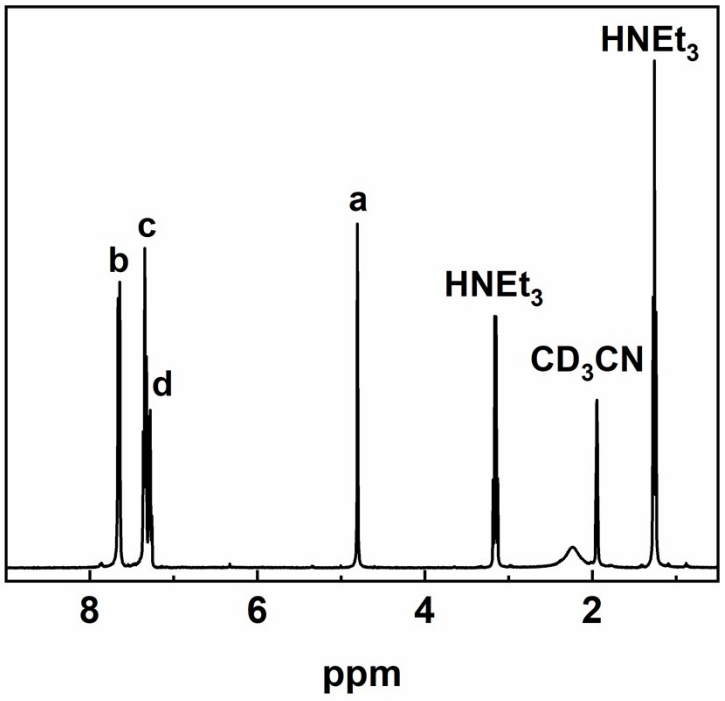

Figure S41. ^{1}H NMR spectrum of $(HNEt_3)[Eu(\mathbf{BTFA})_4]$.

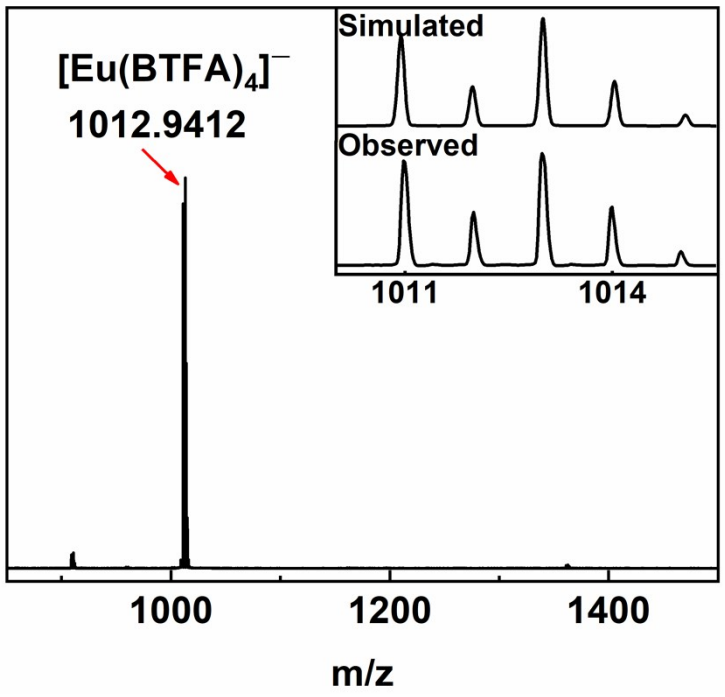

Figure S42. ESI-TOF-MS of $[Eu(\mathbf{BTFA})_4]^-$.

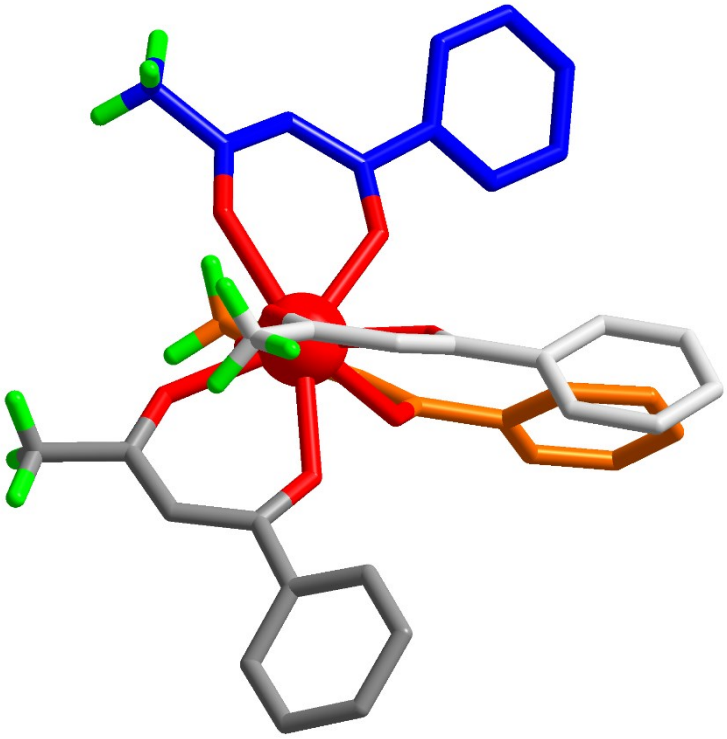

Figure S43. Sparkle/PM3 ground state geometry of $(HNEt_3)[Eu(\mathbf{BTFA})_4]$.

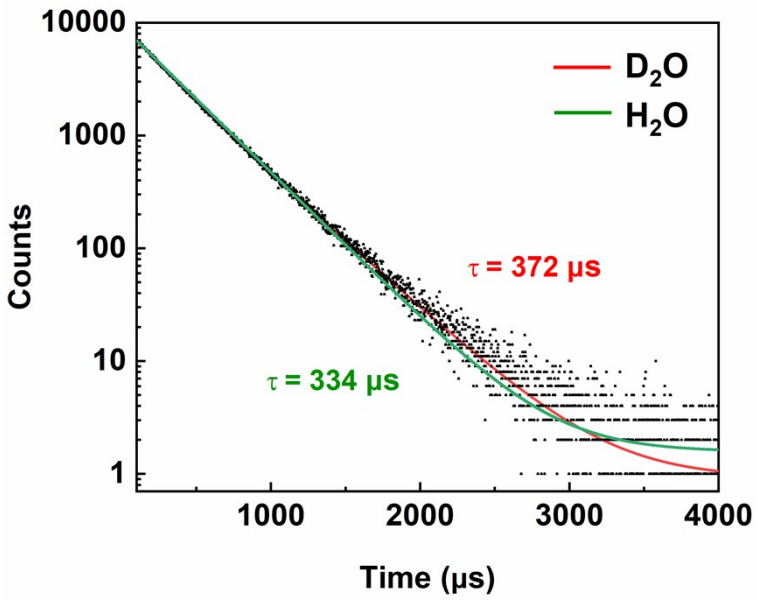

Figure S44. Luminescence decay curves of $(HNEt_3)[Eu(\mathbf{L^1})_2]$ in H_2O (green line) and D_2O (red line).

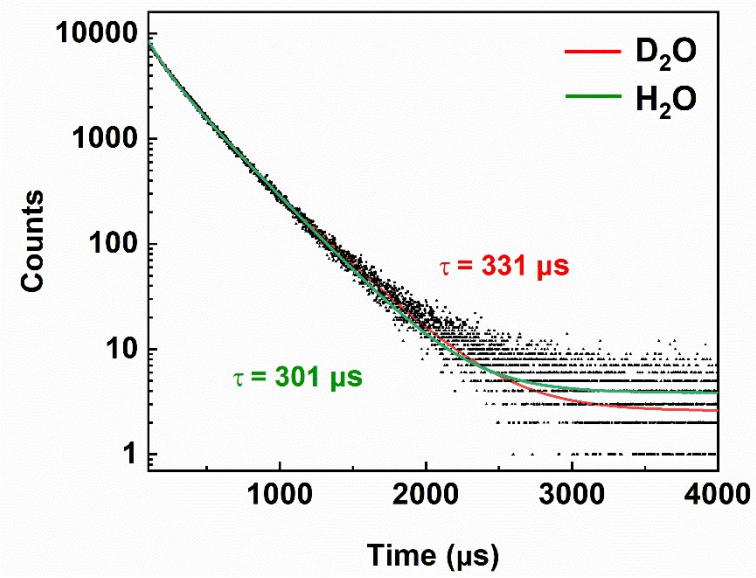

Figure S45. Luminescence decay curves of $(HNEt_3)[Eu(\mathbf{L^2})_2]$ in H_2O (green line) and D_2O (red line).

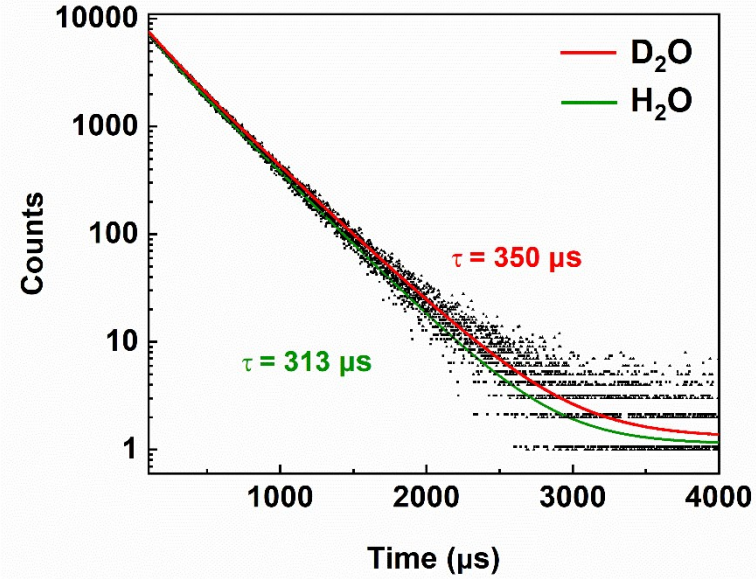

Figure S46. Luminescence decay curves of $(HNEt_3)[Eu(\mathbf{L^3})_2]$ in H_2O (green line) and D_2O (red line).

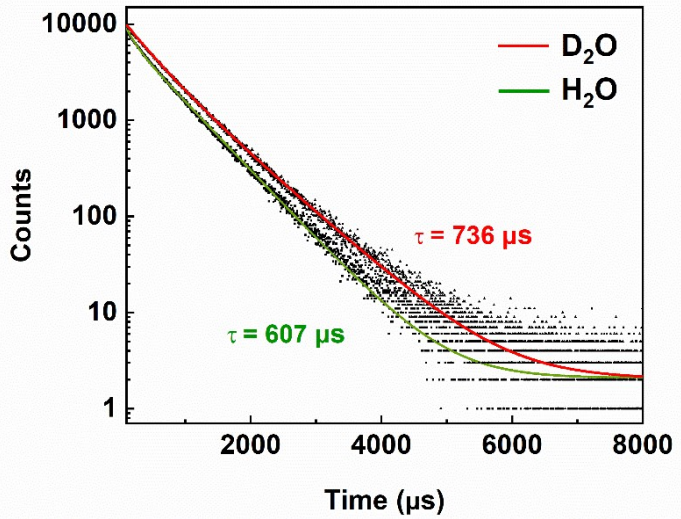

Figure S47. Luminescence decay curves of $(HNEt_3)[Eu(\mathbf{BTFA})_4]$ in H_2O (green line) and D_2O (red line).

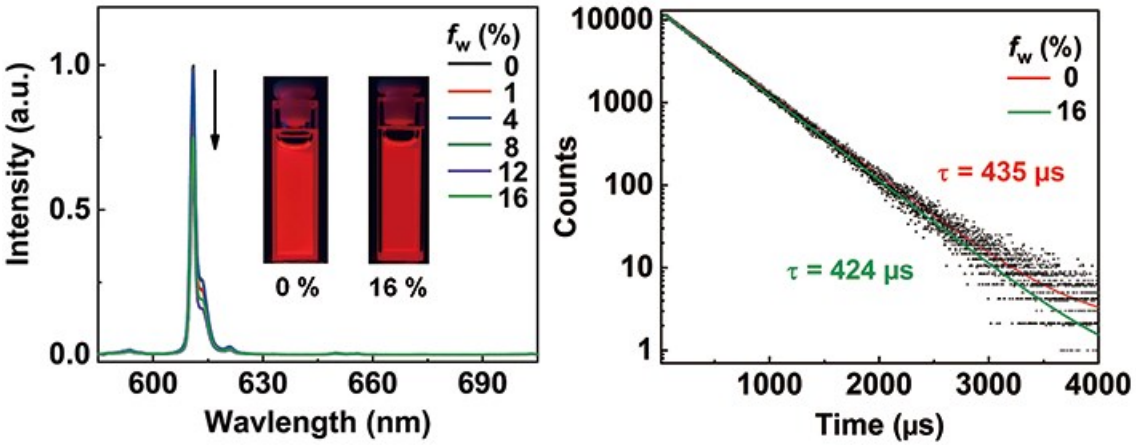

Figure S48. Emission spectra and lifetimes of complexes $(HNEt_3)[Eu(\mathbf{L^2})_2]$ in CH_3CN (λ_{ex} = 330 nm, c = 1.0 × 10^{-5} M; T = 298 k).

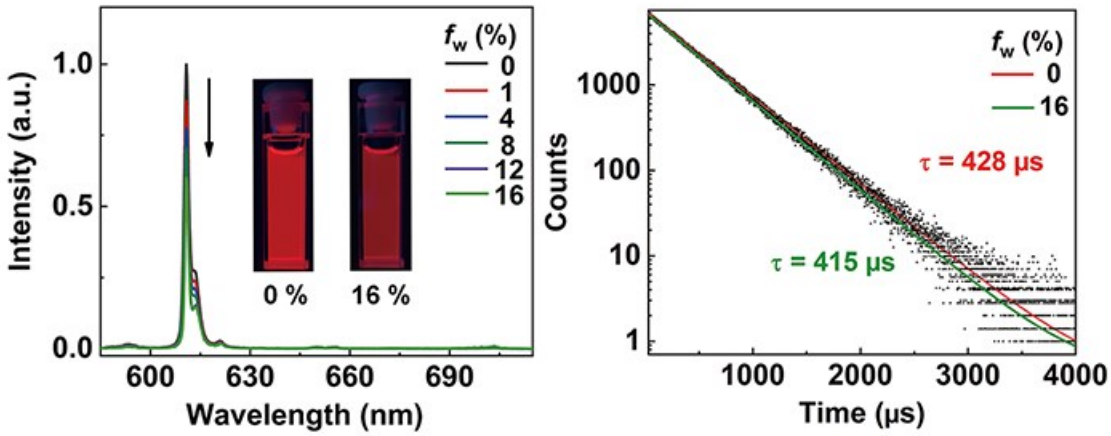

Figure S49. Emission spectra and lifetimes of complexes $(HNEt_3)[Eu(\mathbf{L^3})_2]$ in CH_3CN (λ_{ex} = 330 nm, c = 1.0 × 10^{-5} M; T = 298 k).